

## 중첩의 정리를 이용한 PMSM의 센서리스 제어

\*박현주, 박성준, 김종달, 손무현, 김규섭, 이일천  
동명대학 전기전자계열

### The study on the sensorless PMSM control using the superposition theory

\*Hyun-Ju Park, Sung-Jun Park, Jong-Dai Kim, Mu-Heon Shon, Gyu-Seob Kim, Yil-Chun Lee  
DongMyoung College

**Abstract** - This paper presents a solution to control a PMSM(Permanent Magnet Synchronous Motor) without sensor. The control method is the presented superposition principle. This method of sensorless theory is very simple to compute estimated angle. The use of this system yields enhanced operations, fewer system components, lower system costs, efficient energy control system designs and increased efficiencies. A practical solution is described and its results are given in this study. The performance of a sensorless architecture allows an intelligent approach to reduce the complete system costs of digital motion control applications using the cheaper electrical sensorless motors. This paper deals with an overview of solutions in the sensorless PMSM control applications, whereby the focus will be the new sensorless controller and its applications.

#### 1. Introduction

By the extension of modern automated equipments, the use of servomotor in the industrial and household machines has been on the rapid rise, and the servomotor has been used for the indispensable source of drive in every industrial fields from the industrial robot and all sorts of numerical control machine tools to the household machines.

In a few years ago, most servomotors meant to be DC servomotor using ferrite permanent magnet but they have several weaknesses about frequent inspection and repair and also some problems on high speed operation by reason of brush and commutator. However, AC servomotor using permanent magnet has more complicated control scheme than that of DC servomotor, but has big advantages over both durability and large ratio of power per weight and torque per current because it deals the rectification of DC motor with electrical switching. Recently, high-performance AC motors have been more often used, together with the developments of control technology, semiconductor element and microprocessor. Among them, a permanent magnet synchronizing motor has been generally used in the industrial world. Hereafter, we call it PMSM. It has a disadvantage that properly handled switching is needed to drive AC servomotor and then

position detecting device is also necessary to obtain information on the rotor's position angle. An encoder and a resolver are generally used to detect rotor's position angle, but these exterior mechanical position sensor has not only an economic disadvantage also problem on reliability by sensor's sudden

characteristic change in the worse circumstances. In this case, PMSM has an absolute disadvantage over the machinery used in crash worthiness, corrosion resistance, high temperature, and high humidity. There has been vigorously the study on a sensorless drive for low cost of sensor installation and good robustness on exterior environment.

In this paper, a sensorless control algorithm is proposed to overcome a disadvantage of system using the position sensor. Moreover, its basic theory is based on the superposition principle. That is, motor's state equation is divided into two conditions for analysis: one is the state equation of exciting voltage and phase current in a constraint, the other is the state equation of back EMF(Electromotive Force) and phase current in a short circuit. Based on these analyses, we proposed the new method that it computed simply short circuit current by motor's back EMF in operation and then obtained the information on position angle. It is also proved that the proposed method is presented to be proper by simulation and experimental results.

#### 2. The Modelling of the PMSM

##### 2.1 The Voltage Equation of Motor

The equivalent circuit to analyse numerically 3-phase PMSM with sinusoidal distribution of back EMF is shown in Figure 1. The voltage, current, and impedance equations obtained from this equivalent circuit, that is, the circuit equations are represented as Equation 1.

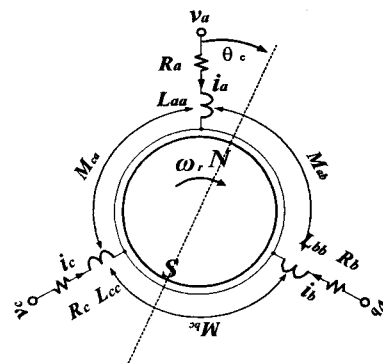


Fig. 1. Three Phase Equivalent circuit of PMSM

$$\begin{bmatrix} v_a \\ v_b \\ v_c \end{bmatrix} = \begin{bmatrix} R_a & 0 & 0 \\ 0 & R_b & 0 \\ 0 & 0 & R_c \end{bmatrix} \begin{bmatrix} i_a \\ i_b \\ i_c \end{bmatrix} + \frac{d}{dt} \begin{bmatrix} L_{aa} & M_{ab} & M_{ac} \\ M_{ba} & L_{bb} & M_{bc} \\ M_{ca} & M_{cb} & L_{cc} \end{bmatrix} \begin{bmatrix} i_a \\ i_b \\ i_c \end{bmatrix} + \begin{bmatrix} e_a \\ e_b \\ e_c \end{bmatrix} \quad (1)$$

, where  $v_a, v_b$  and  $v_c$  are motor's phase voltages at  $a, b, c$ ,  $i_a, i_b$  and  $i_c$  are phase currents at  $a, b, c$ ,  $e_a, e_b$  and  $e_c$  are back EMFs induced from phase stator coil at  $a, b, c$ ,  $R_a, R_b$  and  $R_c$  are the coil resistances at each phase,  $L_{aa}, L_{bb}$  and  $L_{cc}$  are magnetic inductances at each phase,  $M_{ab}, M_{ac}, M_{bc}, M_{ba}, M_{ca}$  and  $M_{cb}$  are mutual inductances between each coil, respectively. The stator coil of PMSM with sinusoidal back EMF as Figure 1 has the symmetric structure at  $120^\circ$  in the same coils and each flux occurred at a phase intercrosses at a half for other phases. In representing motor's cylindrical rotator characteristic, each stator's magnetic inductance depends on the combination of leakage flux and the intercrossing flux shares stator's phases equally.

In addition, this mutual inductance can be regarded as rotator's position and independent variable.

Therefore, each phase has an equal armature coil resistance and armature coil resistances  $R_a, R_b$  and  $R_c$  can be replaced with  $R$ , and mutual inductances between armature coils  $M_{ab}, M_{ac}, M_{bc}, M_{ba}, M_{ca}$  and  $M_{cb}$  can be replaced with  $M$ , armature coil magnetic inductances  $L_{aa}, L_{bb}$  and  $L_{cc}$  can be replaced with  $L_a$ .

The voltage equations of Equation 1 in motor variables obtained from the above can be represented as follows.

$$\begin{bmatrix} v_a \\ v_b \\ v_c \end{bmatrix} = \begin{bmatrix} R + pL_a & -p\frac{M}{2} & -p\frac{M}{2} \\ -p\frac{M}{2} & R + pL_a & -p\frac{M}{2} \\ -p\frac{M}{2} & -p\frac{M}{2} & R + pL_a \end{bmatrix} \begin{bmatrix} i_a \\ i_b \\ i_c \end{bmatrix} + \begin{bmatrix} e_a \\ e_b \\ e_c \end{bmatrix} \quad (2)$$

, where  $p$  is a differentiator ( $p = \frac{d}{dt}$ ).

The stator's magnetic inductance is following the next equation

$$L_a = l + M \quad (3)$$

, where  $l$  represents a motor's leakage inductance. If the motor is connected in the Y form, 3-phase current becomes parallel and then it can be represented as Equation 4.

$$i_a + i_b + i_c = 0 \quad (4)$$

The voltage equation of PMSM from Equation 2,3, and 4 can be shown into simple  $3 \times 3$  matrix form.

$$\begin{bmatrix} v_a \\ v_b \\ v_c \end{bmatrix} = \begin{bmatrix} R + pL & 0 & 0 \\ 0 & R + pL & 0 \\ 0 & 0 & R + pL \end{bmatrix} \begin{bmatrix} i_a \\ i_b \\ i_c \end{bmatrix} + \begin{bmatrix} e_a \\ e_b \\ e_c \end{bmatrix} \quad (5)$$

, where  $L = l + \frac{3}{2}M$ .

each EMF of Equation 5,  $e_a, e_b$  and  $e_c$  are represented as each differentiator of flux intercrossed at phase coils. So, let the maximum value of intercrossing flux  $\lambda_a, \lambda_b$  and  $\lambda_c$  at phase a, b, and c be  $\lambda_m$ , each representation can be as follows.

$$\begin{aligned} \lambda_a &= \lambda_m \cos(\theta_e) \\ \lambda_b &= \lambda_m \cos(\theta_e - \frac{2}{3}\pi) \\ \lambda_c &= \lambda_m \cos(\theta_e + \frac{2}{3}\pi) \end{aligned} \quad (6)$$

, where  $\theta_e$  is a clockwise electrical rotor angle with reference to the stator coil at phase a. The inductive EMF obtained from intercrossing flux of phase coil is represented into Equation 7.

$$\begin{aligned} e_a &= \frac{d}{dt} \lambda_a = -\omega_e \lambda_m \sin(\theta_e) \\ e_b &= \frac{d}{dt} \lambda_b = -\omega_e \lambda_m \sin(\theta_e - \frac{2}{3}\pi) \\ e_c &= \frac{d}{dt} \lambda_c = -\omega_e \lambda_m \sin(\theta_e + \frac{2}{3}\pi) \end{aligned} \quad (7)$$

, where  $\omega_e$  means an rotor's angular velocity and is given as follows.

$$\omega_e = \frac{d}{dt} \theta_e \quad (8)$$

## 2.2 The Coordinates Transformation

It is more convenient to represent 2-phase AC than 3-phase in the voltage and current for understanding of 3-phase PMSM characteristic and derivation of control method

Like the above, the coordinates need to be transformed for different analysis on motor, and it is called to the coordinates transformation. The transformation matrix from 3-phase AC coordinates(a-b-c) to 2-phase AC coordinates( $\alpha$ - $\beta$ ) can be defined as Equation 9 and this transformation results in the motor's equivalent circuit in the fixed 2 axis  $\alpha$ - $\beta$  coordinates at Figure 2.

$$C = \sqrt{\frac{2}{3}} \begin{bmatrix} 1 & -\frac{1}{2} & -\frac{1}{2} \\ 0 & \frac{\sqrt{3}}{2} & -\frac{\sqrt{3}}{2} \end{bmatrix} \quad (9)$$

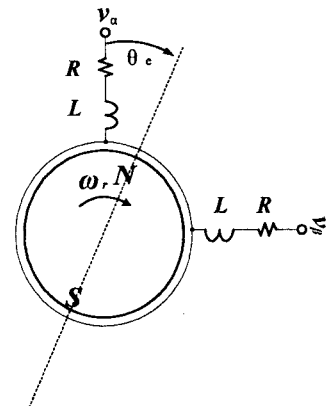


Fig. 2. Two Phase Equivalent circuit of PMSM

The voltage equation of 2-phase equivalent circuit of PMSM in the fixed coordinates is given into Equation 10.

$$\begin{bmatrix} v_\alpha \\ v_\beta \end{bmatrix} = \begin{bmatrix} -R + pL & 0 \\ 0 & -R + pL \end{bmatrix} \begin{bmatrix} i_\alpha \\ i_\beta \end{bmatrix} + \begin{bmatrix} e_\alpha \\ e_\beta \end{bmatrix} \quad (10)$$

This equation can be obtained by multiply the transformation matrix C and the given 3-phase circuit equation together in Equation 5.

, where  $v_\alpha, v_\beta, i_\alpha, i_\beta, e_\alpha$  and  $e_\beta$  are given as follows, respectively.

$$v_\alpha = \sqrt{\frac{2}{3}} (v_a - \frac{v_b}{2} - \frac{v_c}{2}) \quad (11)$$

$$v_\beta = \frac{(v_b - v_c)}{\sqrt{2}}$$

$$i_\alpha = \sqrt{\frac{2}{3}} (i_a - \frac{i_b}{2} - \frac{i_c}{2}) \quad (12)$$

$$i_\beta = \frac{(i_b - i_c)}{\sqrt{2}}$$

$$e_\alpha = -\sqrt{\frac{3}{2}} \omega_e \lambda_m \sin(\theta_e) \quad (13)$$

$$e_\beta = \sqrt{\frac{3}{2}} \omega_e \lambda_m \cos(\theta_e)$$

If the Equation 10 obtained from the 2-axis fixed coordinates( $\alpha-\beta$ ) is rearranged and also represented into the state equation of PMSM, the Equation 14 can be given as follows

$$\begin{bmatrix} \dot{i}_\alpha \\ \dot{i}_\beta \end{bmatrix} = \begin{bmatrix} -\frac{R}{L} & 0 \\ 0 & -\frac{R}{L} \end{bmatrix} \begin{bmatrix} i_\alpha \\ i_\beta \end{bmatrix} + \frac{1}{L} \begin{bmatrix} v_\alpha \\ v_\beta \end{bmatrix} + \frac{1}{L} \begin{bmatrix} e_\alpha \\ e_\beta \end{bmatrix} \quad (14)$$

, where the torque equation is given into Equation 15.

$$T_e = p_{poles} \cdot \lambda_m (-i_\alpha \sin \delta + i_\beta \cos \delta) \quad (15)$$

, where  $\delta$  stands for the angle between rotor and stator.

### 2.3 The Principle of Sensorless PMSM using Superposition Principle

The voltage equation of PMSM given in 2-phase AC coordinates  $\alpha-\beta$  can be represented into the equivalent circuit in the 2 fixed reference axis ( $\alpha-\beta$ ) in Figure 3 and from Equation 10.

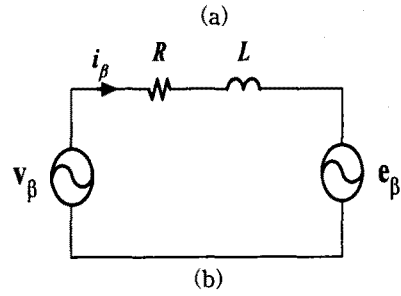
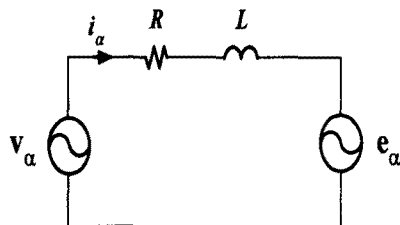


Fig. 3. Equivalent circuit of PMSM by  $\alpha-\beta$  axis  
(a) Equivalent circuit of  $\alpha$  axis  
(b) Equivalent circuit of  $\beta$  axis

As you can see in the circuit of  $\alpha-\beta$  coordinates in Figure 3, the sources forming the motor current are a back EMF voltage and a terminal voltage as two voltage sources. Accordingly, The use of superposition principle which separates into two voltage source can be represented into the equivalent circuit in Figure 4.

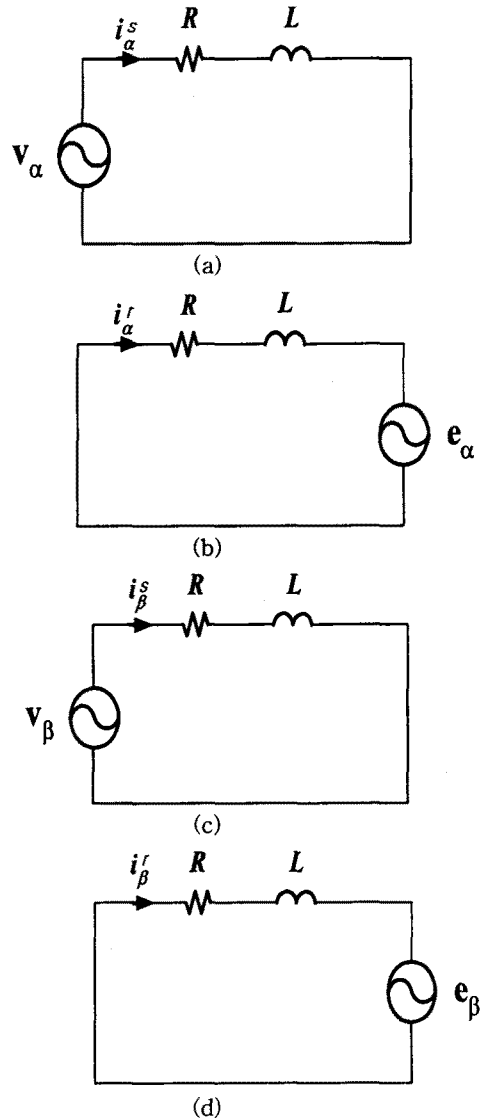


Fig.4 Equivalent circuit of PMSM using superposition principle  
(a)Equivalent circuit of  $\alpha$  axis terminal voltage

- (b)Equivalent circuit of  $\alpha$  axis back EMF voltage
- (c)Equivalent circuit of  $\beta$  axis terminal voltage
- (d)Equivalent circuit of  $\beta$  axis back EMF voltage

According to Figure 4, the source of current through motor can be expressed the inductive EMF term occurred by the phase voltage from inverter and the motor's rotation. The motor current becomes a indispensable factor for overcurrent detection and excellent velocity control of motor. If the motor parameters R and L can be known, the current component by the phase voltage induced from inverter can be found easily. In the equivalent circuit of Figure 4, the circuit represented with the inductive EMF by the motor's rotation and the phase voltage from inverter can be obtained into the following state equation.

$$\begin{bmatrix} \dot{i}_\alpha^s \\ \dot{i}_\beta^s \end{bmatrix} = \begin{bmatrix} -\frac{R}{L} & 0 \\ 0 & -\frac{R}{L} \end{bmatrix} \begin{bmatrix} i_\alpha^s \\ i_\beta^s \end{bmatrix} + \frac{1}{L} \begin{bmatrix} v_\alpha \\ v_\beta \end{bmatrix} \quad (16)$$

$$\begin{bmatrix} \dot{i}_\alpha^r \\ \dot{i}_\beta^r \end{bmatrix} = \begin{bmatrix} -\frac{R}{L} & 0 \\ 0 & -\frac{R}{L} \end{bmatrix} \begin{bmatrix} i_\alpha^r \\ i_\beta^r \end{bmatrix} + \frac{1}{L} \begin{bmatrix} e_\alpha \\ e_\beta \end{bmatrix} \quad (17)$$

The current term by the back EMF can be computed by the difference between the detected real motor current and the current by the phase voltage. Therefore, the current component can be easily obtained, and then this current component of back EMF comes to be directly controlled by the voltage of back EMF. The current term of back EMF, i.e., becomes physical quantity passed through a low-pass filter.

So, the back EMF can be theoretically computed by passing the back EMF's current through high-pass filter, but it needs some techniques for dealing with high-pass filter with weakness at noise. In order to verify back EMF from the current component by back EMF, you can see Equation 17 including the differential term, but come to know that the back EMF term in this equation has lots of switching noise. It is necessary to compute back EMF from numerical solutions of state equation for solving this noise problem. The complete solution of  $\alpha$ -axis back EMF in the state equation of Equation 17 is given as follows.

$$i_\alpha^r(t) = \frac{e_\alpha}{R}(1 - e^{-\frac{R}{L}t}) + i_\alpha^r(0)e^{-\frac{R}{L}t} \quad (18)$$

This solution can be represented into the discrete form as Equation 19.

$$i_\alpha^r(n) \doteq \frac{e(n)}{R}(1 - e^{-\frac{R}{L}\Delta T}) + i_\alpha^r(n-1)e^{-\frac{R}{L}\Delta T} \quad (19)$$

If motor parameter and sampling time are determined, the exponential term of Equation 19 can be dealt with the constant, and its value can be defined as follows.

$$K_T \doteq e^{-\frac{R}{L}\Delta T} \quad (20)$$

Thus, the back EMF term from Equation 19 and 20 can be given as follows.

$$e_\alpha(n) = \frac{R}{(1-K_T)} [i_\alpha^r(n) - K_T i_\alpha^r(n-1)] \quad (21)$$

The solution for back EMF on  $\beta$ -axis can be solved as mentioned above, and if the back EMF can be given on  $\alpha$ - $\beta$  axis, the electrical position angle of rotor can be following that

$$\theta_e = \tan^{-1} \frac{e_\alpha}{e_\beta} \quad (22)$$

The equation obtained from Equation 22, strictly speaking, is also equal to that which passed through high-pass filter. Hence, a simple prediction method is used to remove appropriately the noise component of electrical position angle, and its schematic diagram can be illustrated in Figure 5, where  $Z^{-1}$  means the delay term.

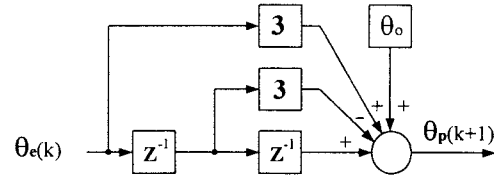


Fig. 5 Schematic diagram of quadratic position prediction

The block diagram of Figure 5 can be numerically expressed as follows, where  $\theta_p(K+1)$  means the prediction value from position angle computed by back EMF to the position angle in the next sampling, where  $\theta_0$  means an initial position angle at a start.

$$\theta_p(k+1) = 3[\theta_e(k) - \theta_e(k-1)] + \theta_e(k-2) + \theta_0 \quad (23)$$

The estimate of rotor position angle can be estimated in this method without reference to a back EMF constant, but the back EMF constant is needed to estimate the motor speed. If the given back EMF on  $\alpha$ - $\beta$  axis, the electrical angular velocity of rotor can be given as follows.

$$\omega_e = \frac{1}{K_E} \sqrt{e_\alpha^2 + e_\beta^2} \quad (24)$$

, where  $K_E$  stands for the back EMF constant.

The information on the number of motor poles is necessary to find mechanical angular velocity from electrical angular velocity. The relation of electrical and mechanical angle according to the number of motor pole can be given as follows.

$$\omega_r = \frac{\omega_e}{p_{poles}} \quad (25)$$

, where  $p_{poles}$  means the motor pole pair.

## 2.4 The Structure of Controller

If transformed from 3-phase fixed coordinates to 2-phase fixed coordinates( $\alpha-\beta$ ) in controlling PMSM, and then the latter transformed into 2-phase rotary coordinates(d-q), all values of variables come to be DC, and also their characteristic to be the same form of DC motor, which makes a control simple. The transformation and inverse transformation from 3-phase fixed coordinates to 2-phase fixed coordinates ( $\alpha-\beta$ ) are following that

$$\begin{bmatrix} f_q^s \\ f_d^s \\ f_o^s \end{bmatrix} = \frac{2}{3} \begin{bmatrix} 0 & \frac{\sqrt{3}}{2} & -\frac{\sqrt{3}}{2} \\ 1 & -\frac{1}{2} & -\frac{1}{2} \\ \frac{1}{2} & \frac{1}{2} & \frac{1}{2} \end{bmatrix} \begin{bmatrix} f_a \\ f_b \\ f_c \end{bmatrix} \quad (26)$$

$$\begin{bmatrix} f_q^s \\ f_d^s \end{bmatrix} = \begin{bmatrix} 0 & \frac{1}{\sqrt{3}} & -\frac{1}{\sqrt{3}} \\ \frac{2}{3} & -\frac{1}{3} & -\frac{1}{3} \end{bmatrix} \begin{bmatrix} f_a \\ f_b \\ f_c \end{bmatrix} \quad (27)$$

The transformation and inverse transformation from 2-phase fixed coordinates to 2-phase rotary coordinates(d-q) are following that

$$\begin{bmatrix} f_q^r \\ f_d^r \end{bmatrix} = \begin{bmatrix} \cos\theta & -\sin\theta \\ \sin\theta & \cos\theta \end{bmatrix} \begin{bmatrix} f_q^s \\ f_d^s \end{bmatrix} \quad (28)$$

$$\begin{bmatrix} f_q^s \\ f_d^s \end{bmatrix} = \begin{bmatrix} \cos\theta & \sin\theta \\ -\sin\theta & \cos\theta \end{bmatrix} \begin{bmatrix} f_q^r \\ f_d^r \end{bmatrix} \quad (29)$$

Figure 6 shows the overall block diagram of proposed algorithm. The motor drive SVPWM(space vector pulse width modulation) in the block diagram uses VSI(voltage source inverter), and the space vector modulation technique is applied in the modulation method. Every algorithm except inverter is also constructed into software to make a hardware briefly. The sampling time is  $200\mu\text{sec}$  in this algorithm.

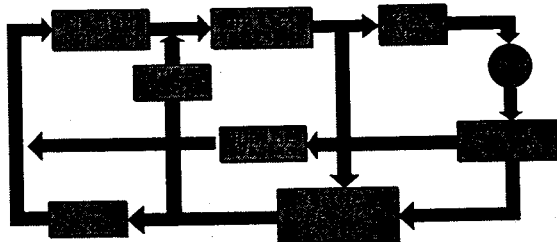


Fig. 6. Diagram of controller

There are DC-LINK voltage and phase current as inputs to realize this algorithm. After transforming the 3-phase fixed coordinates into 2-phase fixed coordinates by using these inputs, first the rotor position angle and velocity is estimated and then converted into 2-phase rotary coordinates for control.

### 3. Experimental Results and Analyses

#### 3.1 The Parameter Estimation of PMSM

Figure 7(a) shows the rotor of motor for a washing machine, and Figure 7(b) shows the stator of motor. As you can see in figure, Motor with 48 poles is designed for a low speed.

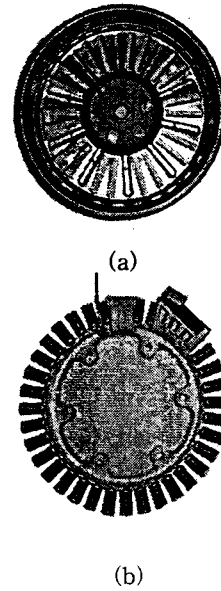


Fig. 7. Rotor & stator of PMSM at experiment  
(a) Rotor (b) Stator

Figure 8 shows the measured back EMF waveforms of PMSM into a washing machine, where it can be found that this back EMF has better sine waves.

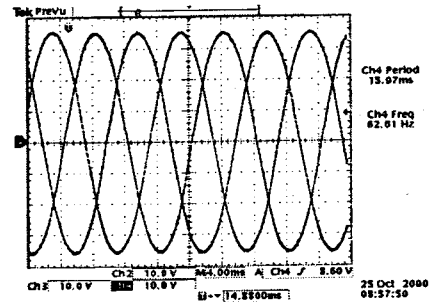


Fig. 8. back EMF waveforms of a, b, c phase

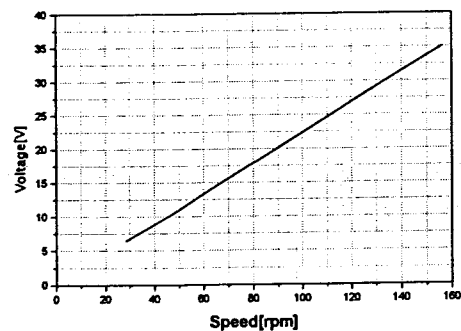


Fig. 9. back EMF of PMSM

Figure 9 illustrates the relation between rotation speed and back EMF in varying rotation speed of motor. It can be, as you can see in Figure 9, found that the ratio value of back EMF to rotation speed of motor has nearly a linearity over 98 %. Therefore, the speed can be easily solved by multiplying the back EMF constant  $K_E$ , if the back EMF is computed. When DC voltage 24V is, moreover, forced

to measure resistance  $R$  and inductance  $L$  as important parameters for sensorless control, the following current waveform is shown in Figure 10. The values of  $R$  and  $L$  can be found by analysing the rise curve of the current waveform at each phase of motor in Figure 10.

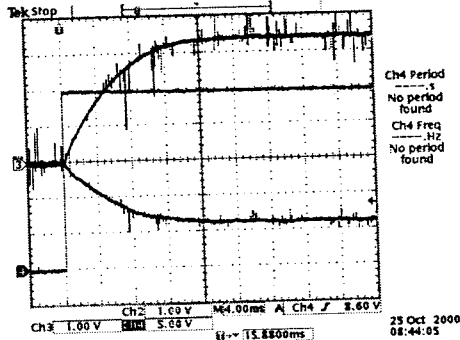


Fig. 10. Current waveform at step DC voltage

This experiments is accomplished on the magnetic field phase of PMSM with the measured parameters in Table 1.

Table 2 The measured motor parameters

Winding resistance	1.981[ $\Omega$ ]
Winding inductance	10.8[mH]
EMF constant	0.224[rpm/V]
Number of poles	24 poles
Rated current	6.0[A]
Rated Speed	600[rpm]

Figure 11 shows the waveform comparing the solution of state equation in Equation 16 with real current value by changing the terminal voltage in a motor constraint, i.e., when the back EMF is equal to zero in order to verify  $R$  and  $L$  measured in the above.

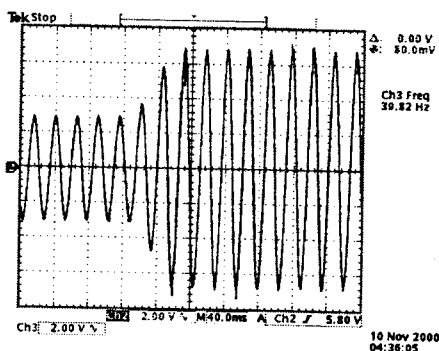


Fig. 11. Motor current and estimate current waveforms(Constrained)

In the above figure, it can be known that it estimates almost perfectly to real current with all the changes of input voltage. It shows that the value of  $R$  and  $L$  among the motor parameters are accurate.

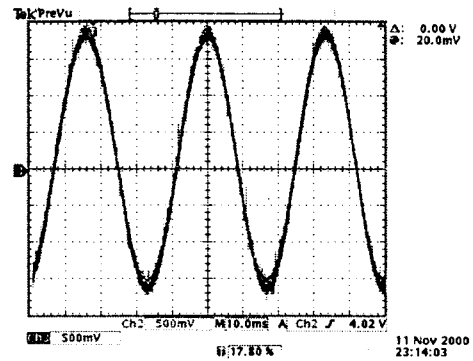


Fig. 12. Motor current and estimate current waveforms(in a short circuit)

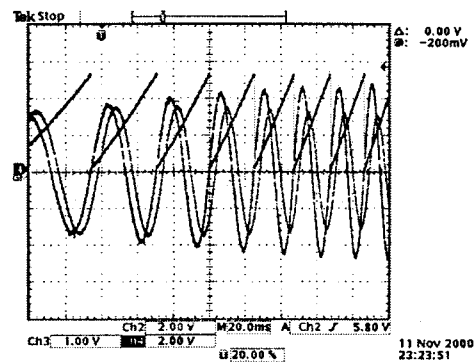


Fig. 13. Rotor current, back EMF & position of rotor

When making a short at the motor terminal, and then driving the motor with exterior power, the motor current and the estimate current waveforms are shown in Figure 12. The terminal current, the estimate back EMF and the electrical rotor position detected from encoder are shown in Figure 13. It can be, as you can see in Figure 13, known that it can estimate a better position with coincidence in  $\alpha$ -axis back EMF and the zero point of rotor.

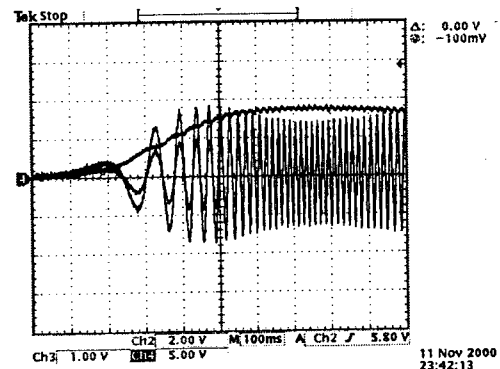


Fig. 14. Rotor current & estimate current at external start

Figure 14 shows the terminal current, the estimate current and the estimate speed in driving by the exterior motor under the same condition of Figure 13.

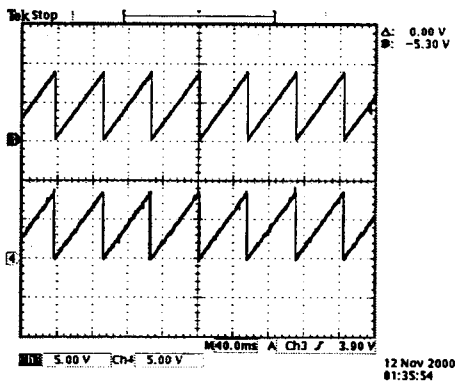


Fig. 15. Real and estimate angle

Figure 15 shows real rotor position and the estimate rotor position when the sensorless control is achieved by the proposed algorithm. It can be, as can be seen in figure, found that the estimate position of rotor is better achieved.

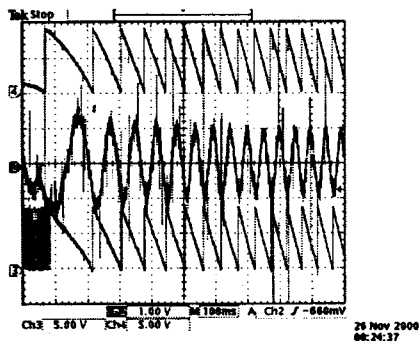


Fig. 16. Real & estimate angle at a start

Figure 16 shows the terminal current, the estimate angle and the real angle in driving by sensorless control. Since a cylindrical PMSM has a fixed inductance regardless of the rotor position, no information can be obtained about the initial position. Therefore, it moves with the zero initial position and then its mobile characteristic is somewhat changed by the initial position of rotor.

#### 4. Conclusions

In this paper, a method of sensorless control algorithm based on superposition principle is proposed. After the state equation of motor is separated into two state equations in each constraint and short circuit, they are analysed. Based on this analysis, the back EMF component can be analysed by simply computing the short circuit current by motor's back EMF component in operation, whereby a position angle computation technique is proposed. The experiment using a PMSM in a washing machine is made to verify a properness of control algorithm and then results in the following characteristics.

1. In this control algorithm, the rotor's position can be estimated without an information about back EMF constant.
2. Even if R and L values vary up to 30%, a stable sensorless control is possible.
3. the mobile characteristic somewhat can be

changed by the initial rotor position at a start.

When the rotor position is aligned to fix the initial position, the alignment characteristic can be different by the rotor position.

If this control algorithm is applied to the PMSM, an improvement in productivity and an increase on durability is expected by not only the performance improvement of products but also the simple structure. In addition, even though a motor characteristic or a manufacturing maker is changed, the changed system can be accessed by using the known motor parameters.

#### [References]

- [1] T. M. Jahns, "Torque production in permanent magnet synchronous motor drives with rectangular current excitation", *IEEE Trans. Indust. Applicat.*, Vol. 20, No. 4, pp. 803-813, July/June 1984.
- [2] H. R. Bolton and R. A. Ashen, "Influence of motor design and feed-current waveform on torque ripple in brushless DC drive", *Proc. of IEE*, Vol. 131, Part B, No. 3, pp. 82-90, May 1984.
- [3] D. Hanselman, J. Y. Hung and M. Keshura, "Torque ripple analysis in brushless permanent magnet motor drive", *Proc. of ICEM 92*, Manchester, UK, pp.823-827, Sept. 1992.
- [4] H. Le-Huy, R. Perret and R. Feuillet, "Minimization of torque ripple in brushless DC motor drive", *IEEE Trans. Indust. Applicat.*, Vol. 22, No. 4, pp. 748-755, July/Aug. 1986.
- [5] J. Y. Hung and Z. Ding, "Minimization of torque ripple in permanent magnet motors", *Proc. 18th IEEE Industrial Electronics Conf.*, San Diego, CA, pp.459-463, Nov. 1992.
- [6] D. C. Hanselman, "Minimum Torque Ripple, Maximum Efficiency Excitation of Brushless Permanent Magnet Motors", *IEEE Trans. Ind. Applicat.*, Vol. 41, No. 3, pp. 292-300, June. 1994.